Nanofabricated solid immersion lenses registered to single emitters in diamond

L. Marseglia,[1,a)] J. P. Hadden,[1] A. C. Stanley-Clarke,[1] J. P. Harrison,[1] B. Patton,[1]
Y.-L. D. Ho,[1] B. Naydenov,[2] F. Jelezko,[2] J. Meijer,[3] P. R. Dolan,[4] J. M. Smith,[4] J. G. Rarity,[4]
and J. L. O'Brien[1]

[1]*Department of Electrical and Electronic Engineering, H. H. Wills Physics Laboratory, Centre for Quantum Photonics, University of Bristol, Bristol BS8 1UB, United Kingdom*
[2]*3 Physikalisches Institut and Research Center SCoPE, Universität Stuttgart, 70569 Stuttgart, Germany*
[3]*Ruhr-Universität Bochum, 44801 Bochum, Germany*
[4]*Department of Materials, University of Oxford, Oxford OX1 3PH, United Kingdom*

We describe a technique for fabricating micro- and nanostructures incorporating fluorescent defects in diamond with a positional accuracy better than hundreds of nanometers. Using confocal fluorescence microscopy and focused ion beam etching, we initially locate a suitable defect with respect to registration marks on the diamond surface then etch a structure using these coordinates. We demonstrate the technique by etching an 8 μm diameter hemisphere positioned with single negatively charged nitrogen-vacancy defect lies at its origin. Direct comparison of the fluorescence photon count rate before and after fabrication shows an eightfold increase due to the presence of the hemisphere. © *2011 American Institute of Physics*. [doi:10.1063/1.3573870]

Diamond has seen a resurgence of interest in its optically active defects (color centers), notably the nitrogen-vacancy (NV) center and most recently, various chromium-associated centers,[1] all of which show promise as single photon sources.[2–4] The center consists of a substitutional nitrogen atom adjacent to a carbon atom vacancy.[5,6] The negatively charged NV color center NV[−] is a spin active defect with a long spin lifetime at room temperature.[7,8] The nondegeneracy of the ground state multiplet allows the use of spectrally high resolution resonant excitation as a direct probe of the spin state.

In order to use the spin state in a quantum information processing (QIP) device, or in quantum enhanced metrology (QEM), it is necessary to be able to use the information of the spin state before the spin has decohered. One of the current rate-limiting steps for the development of diamond-based technology is related to the efficiency with which photons can be coupled from the optically active defect into the collection mode, or analysis channel, of the QIP or QEM device. The high refractive index mismatch at any diamond-air interfaces limits the solid angle from which photons can be collected due to refraction and adds additional Fresnel losses and strong spherical aberration which must be corrected for in the subsequent optical design. One solution would be to use defects embedded in a meso- or macroscopic diamond sample and to directly improve the coupling efficiency from a planar surface by fabricating structures such as solid immersion lenses (SILs) (Refs. 9 and 10) or photonic wire microcavities.[11]

Hemispherical SILs are interesting structures because they geometrically avoid any refraction at the diamond-air interface; if we consider a color center placed at the origin of a hemisperical diamond surface the fluorescent light coming out is perpendicular to the surface over the full 2π solid angle of the hemisphere. Recently,[9] we reported an increase

by a factor of 10 in the saturated count rate from a single NV[−] center using such structures. A focused ion beam (FIB) milling technique was used to etch hemispheres of 5 μm diameter into the surface of synthetic diamond material that had a moderate density of as-grown NV[−] centers. A number of these SILs were found to contain a single NV[−] center and, comparing the fluorescence intensity with the typical intensity of single NV[−]s in an unetched region, up to an order of magnitude improvement in photon collection was measured. However, in this sample a large fraction of the SILs fabricated were empty of NV[−] centers. As such, we etched as many SILs as time permitted and then examined them to find one suitably located about an NV[−] center. It is clear that for scalability purposes, a different approach is required.

In this letter, we demonstrate a protocol for fabricating SILs incorporating single NV[−] centers in diamond in a predetermined, rather than postselected, way. Registration marks on the diamond surface that can be identified in our confocal fluorescence microscope allowed us to initially locate and then characterize particular NV[−] centers in a robust and repeatable way. These registration marks, also visible in the FIB system, allowed us to etch a SIL with a single NV[−] center located precisely at the origin of the hemisphere. This approach eliminates the randomness of our previous approach and, importantly, allows us to make a direct comparison of the same NV[−] center before and after the FIB-etching process.

The sample used in this work was a $5 \times 5 \times 1$ mm single crystal type IIa diamond grown by chemical vapor deposition (CVD) containing substitutional nitrogen impurities below the detection limit (element six). Nitrogen implantation was performed over a total area of $\sim 1.6 \times 0.2$ mm in a grid pattern with 10 μm separation between implanted spots. An energy of 6 MeV was used so that the resulting implantation depth was ~ 4 μm. The implanted area received an average nitrogen dose of 10 ions per implanted spot. Following implantation, the sample was annealed at 800 °C for 2 h. At

---

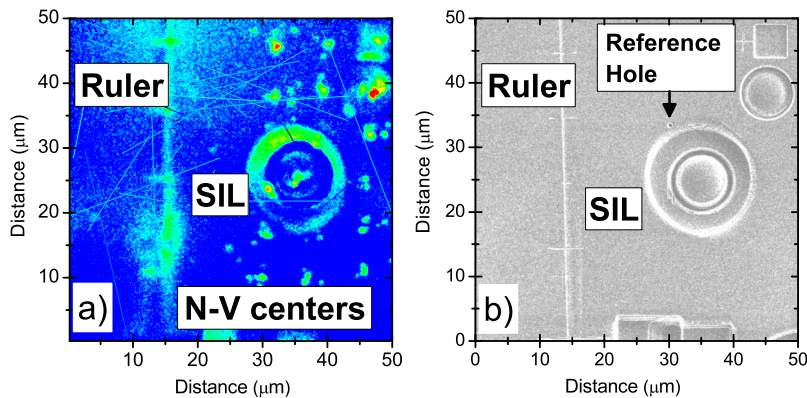a)Electronic mail: luca.marseglia@bristol.ac.uk.

FIG. 1. (Color online) Confocal scanning image at a depth of 4 μm. (a) The array of implanted NV$^-$ centers and the SIL are both visible on the right of the image. Also visible, on the left, is the defocused image of the ruler etched into the surface of the sample. (b) FIB image of the processed area on our sample. Highlighted are the etched ruler used for coarse positioning, the reference hole drilled for accurate location of the defect of interest, and the SIL described in the text. The structures in the top right of the image are test objects for calibration of the etching process.

this temperature, carbon-vacancies (created by the ion implantation) become mobile in the diamond lattice and have some probability of forming NV$^-$ centers with the implanted nitrogen atoms.

In order to observe the array of implanted NV$^-$ centers (Fig. 1), we used a confocal fluorescence microscope system in the reflection geometry. In analysis mode, the fluorescence signal can be directed either to an optical spectrometer for spectral analysis, or to two SPADs in a Hanbury-Brown and Twiss configuration to measure the second order intensity correlation function $g^2(\tau)$.

Having a suitable sample, we next searched for single NV$^-$ centers by optically scanning across the entire implanted array. Once we have cataloged any single NV$^-$ centers we need to be able to precisely locate their position in order to correctly fabricate a SIL.

We used a 30 keV gallium FIB system (see our previous work[9] for details) for fabrication. The FIB can also be used for imaging by rastering the ion beam at a low current and detecting the secondary electron emission. As diamond is dielectric and will build up charge during the FIB process, resulting in degradation of the FIB accuracy; a thin layer of platinum was deposited on the diamond surface before etching to minimize these effects.

In order to etch structures precisely over color centers it is necessary to be able to map between the fluorescence images of the NV$^-$ centers and the FIB images of the diamond surface. To do this we etch registration marks that are identifiable in fluorescence using the confocal microscope. The position of the implanted region within the overall diamond slab was known with an accuracy of tens of microns, so the initial step in correlating the optical and FIB images of the sample was to use the FIB to etch a "ruler" just outside the implanted region. We are then able to search for and catalog the position of single NV$^-$-centers relative to the ruler using the confocal microscope [see Fig. 1(a)].

A cautious approach was adopted because the ion beam must also be used to image the sample and it was unclear if damage and/or implantation from the gallium, even at low flux (but not low energy), might affect the implanted single NV$^-$ centers or contribute additional unwanted fluorescence. Great care was taken to clean the diamond before each step in the fabrication process, primarily to remove surface gallium, platinum, sp^2 carbon, and organic contaminants. The cleaning procedure involved used acetone to remove dustlike contaminants, followed by an isopropanol clean to remove the acetone and a distilled water rinse for the isopropanol. An acid cleaning is then performed in 100 ml of sulfuric acid

and 5 mg of potassium nitrate for 20 min at 200 °C to remove more strongly bonded contaminants. After three iterations of the acid boil, the sample is rinsed thoroughly in deionized water. Having noted that imaging with gallium does not decrease the fluorescence of the NV$^-$ centers, we can then iterate the process to draw successively more precise reference marks with the FIB while continuing to minimize the area of the single NV$^-$ zone exposed to gallium irradiation.

Once we are satisfied that we have a suitable crude correlation between the images from the FIB and the optical scans by using the etched ruler, we make an additional, and final, reference mark to precisely locate the single NV$^-$ by etching a hole of 300 nm radius $\sim$10 μm from it. Figure 1(b) shows a FIB image of the FIB-etched ruler, the SIL and the final reference dot we etched close to the single NV$^-$ center.

The SIL structure itself was etched in two stages: we initially etched an annular trench of 20 μm outer diameter, inner diameter of 8 and 4 μm deep, and subsequently, an 8 μm diameter hemisphere centered in the trench (i.e., the top of the SIL is now level with the surface of the bulk diamond). In both stages, a test structure was initially etched outside of the implanted zone. This is because, even with the platinum deposition, there are still charging effects that cause the FIB to be deflected. To compensate for this problem, we attempt to etch our test structure (trench or hemisphere) with its center at known coordinates with reference to the FIB field of view. Then we measure the difference between these coordinates and the actual center of the etched structure. We can use this offset value when we etch the real structure to place the color center at the appropriate position within the FIB field of view.

The results of this SIL fabrication process are shown in Fig. 2(a) and Fig. 2(c). In Fig. 2(d), we show a confocal image of the NV$^-$ with additional structure in the background noise showing the geometry of the SIL. This image shows our ability to center the NV$^-$ on the SIL, it is also worth noting that the SIL imparts an effective magnification equivalent to the refractive index n=2.4 of the diamond, thus making the apparent radial centering error of 500 nm translate to an actual positioning error of 210 nm. This is within the calculated error[12] for which the SIL operates at greater than 90% of the maximum efficiency. At the center of the trench a brightly fluorescent spot can be seen clearly. The second order autocorrelation function measurement, shown in Fig. 2(b), again confirms single NV$^-$ emission. We normalized and corrected the data for background as described
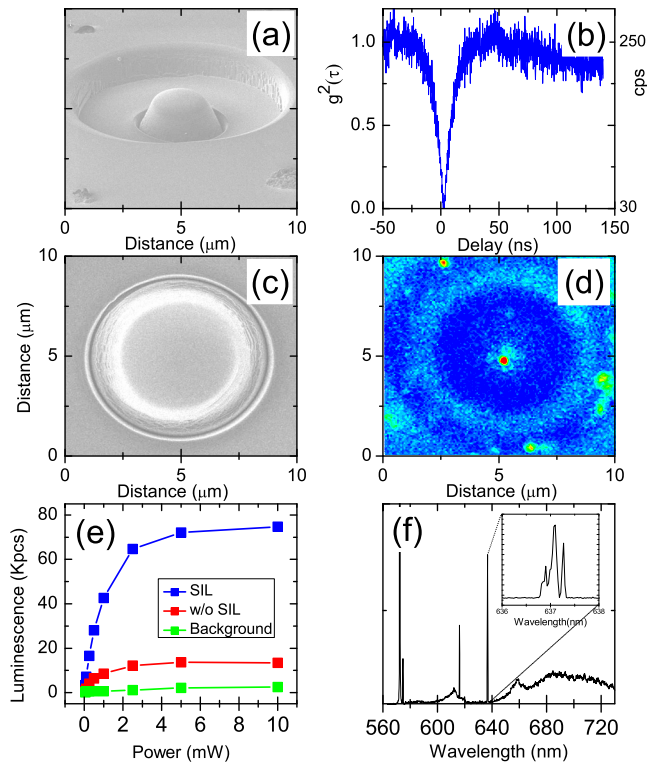
FIG. 2. (Color online) (a) 45° tilted FIB image of the etched SIL on the single NV$^-$ center, (b) second order autocorrelation function $g^2(\tau)$ (left axes:corrected coincidence counts, right axes:uncorrected coincidence counts) of the located single NV$^-$ center inside the fabricated SIL, taken at the excitation power of 0.1 mW, (c) FIB image of the etched SIL on the single NV$^-$ center, (d) photoluminescence image of the SIL with the enhanced emission from the NV$^-$ center taken at temperature T=4.2 K, (e) comparison of the different photoluminescence count rates as function of the laser intensity, (f) spectrum taken at temperature T=4.2 K showing Raman line and the single NV$^-$ center.

by Beveratos.[2] The photon count rate as a function of excitation power was measured before and after etching the SIL, allowing us to make a direct comparison of the saturation curves for the single NV$^-$ [Fig. 2(e)]. From this, we see that the saturated photon count rate has increased by a factor of 8.

We also performed spectroscopy of the defect at liquid helium temperatures to observe the effect of the SIL on the NV$^-$. Figure 2(f) shows a typical spectrum. The sharp line at 574 nm is the first order Raman signal from the 532 nm excitation source and is accompanied by a broad second-order Raman peak centered at 615 nm. The NV^0 peak at 576 nm is clearly visible, as is the NV$^-$ emission with its ZPL at 637 nm and the spectrally broad phonon-assisted emission to longer wavelengths. The inset to this figure shows a high resolution spectrum of the ZPL. The splitting evident is consistent with spectra from other implanted NV$^-$ centers and is likely due to state mixing in the excited state due to strain from vacancies generated in the implantation procedure and does not result from the FIB process.

Summarizing, we have demonstrated a technique that allows us to precisely locate, with positional accuracy limited by the optical resolution and pointing accuracy, a single NV$^-$ center in diamond and fabricate a hemispherical SIL on it. The process is independent of the color center studied and will allow us in the future the possibility of creating SILs placed on different color centers, such as chromium centers. The same technique could be also used to create different structures, such as photonic crystal cavities, etched exactly onto the place of the emitter allowing us to measure the coupling between the NV$^-$ and the photonic crystal cavity. This type of structure would be suitable, for example, to perform quantum non demolition spin readout measurement as we have recently shown theoretically in another work,[13] where we demonstrated that spin readout with a small number of photons could be achieved by placing the NV$^-$ center in a subwavelength scale microcavity with a moderate Q-factor. The technique we reported here opens further routes to the fabrication of nanoscale and microscale structures, precisely aligned to single defects for a wide range of applications.

[1] I. Aharonovich, S. Castelletto, B. C. Johnson, J. C. McCallum, D. A. Simpson, A. D. Greentree, and S. Prawer, Phys. Rev. B **81**, 121201 (2010).

[2] A. Beveratos, S. Kuhn, R. Brouri, T. Gacoin, J. P. Poizat, and P. Grangier, Eur. Phys. J. D **18**, 191 (2002).

[3] W. L. Barnes, G. Bjork, J. M. Gerard, P. Jonsson, J. A. E. Wasey, P. T. Worthing, and V. Zwiller, Eur. Phys. J. D **18**, 197 (2002).

[4] E. Ampem-Lassen, D. A. Simpson, B. C. Gibson, S. Trpkovski, F. M. Hossain, S. T. Huntington, K. Ganesan, L. C. L. Hollenberg, and S. Prawer, Opt. Express **17**, 11287 (2009).

[5] G. Davies and M. F. Hamer, Proc. R. Soc. London, Ser. A **348**, 285 (1976).

[6] M. V. G. Dutt, L. Childress, L. Jiang, E. Togan, J. Maze, F. Jelezko, A. S. Zibrov, P. R. Hemmer, and M. D. Lukin, Science **316**, 1312 (2007).

[7] E. van Oortt, N. B. Manson, and M. Glasbeekt, J. Phys. C **21**, 4385 (1988).

[8] R. J. Epstein, F. M. Mendoza, Y. K. Kato, and D. D. Awshalom, Nat. Phys. **1**, 94 (2005).

[9] J. P. Hadden, J. P. Harrison, A. C. Stanley-Clarke, L. Marseglia, Y.-L. D. Ho, B. R. Patton, J. L. O'Brien, and J. G. Rarity, Appl. Phys. Lett. **97**, 241901 (2010).

[10] P. Siyushev, F. Kaiser, V. Jacques, I. Gerhardt, S. Bischof, H. Fedder, J. Dodson, M. Markham, D. Twitchen, F. Jelezko, and J. Wrachtrup, Appl. Phys. Lett. **97**, 241902 (2010).

[11] T. M. Babinec, B. J. M. Hausmann, M. Khan, Y. Zhang, J. R. Maze, P. R. Hemmer, and M. Loncar, Nat. Nanotechnol. **5**, 195 (2010).

[12] S. Castelletto, J. P. Harrison, L. Marseglia, A. C. Stanley-Clarke, B. C. Gibson, B. A. Fairchild, J. P. Hadden, Y.-L. D. Ho, M. P. Hiscocks, K. Ganesan, S. T. Huntington, F. Ladouceur, A. D. Greentree, S. Prawer, J. L. O'Brien, and J. G. Rarity, New J. Phys. **13**, 025020 (2011).

[13] A. Young, C. Y. Hu, L. Marseglia, J. P. Harrison, J. L. O'Brien, and J. G. Rarity, New J. Phys. **11**, 013007 (2009).